Radboud University Nijmegen

Faculty of Science

Two-dimensional Quantum Gravity on discrete flat annuli

Discussing the properties of random two-dimensional flat surfaces

Thesis BSc Physics and Astronomy

Author:
Isa Vervuurt

Supervisors:
dr. Timothy Budd
Bart Zonneveld

Second reader:
prof. dr. Wim Beenakker

March 2025

Abstract

There is still no complete theory for quantum gravity. One of the promising approaches is Jackiw-Teilboim (JT) gravity in a two-dimensional toy model. Inspired by this, we will look at models with finite, discretized boundaries. With the assumption of a flat inside, we get flat objects such as disks and annuli, which are allowed to self-overlap. The problem is now reduced to counting these self-overlapping flat disks and annuli. These flat disks have recently been studied by Budd [1], however, certain methods are not applicable for surfaces with higher topologies, like annuli. We will show that the number of annuli created from a given side Z' does also depend on the moduli space of each created annulus. Which is in contrary to disks, where the number only depends on the cardinality of the given side set.

At last, we will use the bijection between annuli and closed walks in $\mathbb{R}^2$. We found that in a closed walk the winding area which corresponds to the turning number of the annulus is the moduli space of each annulus, and make an attempt to find the ratio between the length of the curves of an annulus, which is interesting to look at the closed walk approaches a Brownian bridge. Finally, we will briefly discuss the possibilities to generalizing certain methods to higher topologies.

Contents

1 Introduction

At the beginning of the last century, Albert Einstein published his theory on general relativity. He described the curvature of spacetime due to heavy bodies in the universe. His theory has now been verified experimentally in various ways. However, there does not yet exist a way of combining his theory with quantum mechanics, since his theory is completely deterministic. Trying to describe gravity on quantum-mechanical scales is currently one of the main open research questions in physics. Physicists want to find unification of the theories of general relativity and quantum mechanics. The search for this unification theory, called *quantum gravity*. This theory tries to combine the non-deterministic component of quantum mechanics with gravity.

One of the suggested approaches is looking at the geometries of spacetimes at scales where quantum mechanical effects are not negligible. In JT-gravity, these geometries become random surfaces. A proposal of Ferrari in these papers [6, 7], is to look at surfaces with boundaries that do not immediately diverge. Which we will discuss further in chapter 2

As quantum mechanics is non-deterministic, these boundaries are random and therefore, need a statistical approach; hence, our goal is to be able to sum over all possible geometries. This has already been done for surfaces with one boundary (disks) [1]. These methods have not been written out explicitly before; we will do this in chapter 3. In chapter 4 we will look at the mathematical properties of surfaces with a second boundary and try to sum over those geometries as well, while we use certain methods from chapter 3. Eventually we will show the bijection between a closed random walk and an annulus.

2 Background

2.1 General relativity and quantum mechanics

In general relativity, spacetime is curved due to the presence of energy, which then influences matter. Einstein described this in his equations:

$$R_{\mu\nu} - \frac{1}{2}Rg_{\mu\nu} = \frac{8\pi G}{c^4}T_{\mu\nu}, \tag{1}$$

which are also known as the Einstein field equations, where R is the Ricci scalar, and $R_{\mu\nu}$ the Ricci tensor. $T_{\mu\nu}$ is the stress-energy tensor, which describes the density and flux of energy. The Ricci tensor and scalar are functions of $g_{\mu\nu}$, which is called the metric, it describes the distance between points according to $ds^2 = g_{\mu\nu}dx^\mu dx^\nu$, therefore, it tells us something about the geometry of a spacetime [**?**].

When looking at Planck scales, quantum mechanical effects must be taken into account. In contrast to general relativity, quantum mechanics is based on probabilities. Quantum mechanics is quite often described by the Schrödinger equation. However, in our case, the path integral formalism by Feynman is more useful [9]. This formalism replaces the classical approach of following the trajectory of a single particle by a sum over all possible trajectories. This can be written as the following integral:

$$Z = \int e^{\frac{i}{\hbar}S(x(t))}\ \mathcal{D}x. \tag{2}$$

This integral sums over all possible paths, which is denoted by $\mathcal{D}x$. This integral is infinite-dimensional over all possible paths x a particle can take between two points. Each path has a corresponding Feynman weight $e^{\frac{i}{\hbar}S(x(t))}$, defined by the action S. By applying a Wick rotation, which analytically continues the time variable to the complex line, we set $\tau = it$. The integral is reduced to

$$Z = \int e^{\frac{-1}{\hbar}S_E(x(\tau))}\ \mathcal{D}x, \tag{3}$$

which can be interpreted as a partition sum where each possible path is given a Boltzmann weight, $e^{\frac{i}{\hbar}S_E(x(\tau))}$. The integrand is now real and positive, therefore, it can be seen as a Boltzmann distribution. The Wick rotation also causes the original Minkowski metric to simplify to a Euclidean metric. This is a great benefit when using the path integral formalism.

2.2 Quantum Gravity

We can now look at a theory that attempts to describes gravity at Planck scales. This theory is called *Euclidean Quantum Gravity*. In general relativity, the system is described by the metric $g_{\mu\nu}$ instead of the path of particles. This implies that the integral of the previous section changes its differential to as sum of all possible geometries, $\mathcal{D}g$. This are all possible Euclidean metrics, that cannot be transformed to each other using coordinate transformations. [9, chapter 6]

$$Z = \int e^{\frac{-1}{\hbar}S_{EH}(g_{ab})}\ \mathcal{D}g_{ab}, \tag{4}$$

Due to the Wick rotation, our metric is now Euclidean, this is indicated by the use of the indices a and b. The action S_{EH} is to be the Euclidean Einstein-Hilbert action. This can be derived from the Einstein equations (1) and is given by:

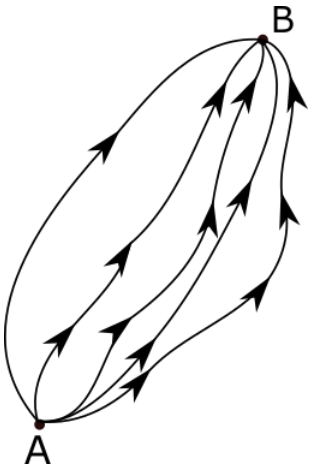

Figure 1: Five of the infinitely many possible paths between two points, a visual explanation of the path-integral formalism. *Source: Wikipedia, path integral formulation*

$$S_{EH} = \int \sqrt{g}\, R \, \mathrm{d}^d x. \tag{5}$$

Now we have found the starting point of Euclidean Quantum Gravity. However, we immediately encounter a problem: the action defined above is unbounded for dimensions higher than two. This is known as the *conformal factor problem* [2]. However, we are more interested in finding a good definition of $\mathcal{D}g_{ab}$. Because if we see the integrand as a Boltzmann distribution, we have to sum over all possible metrics. Since there are infinitely many possible metrics, we need to establish a clearer way to define this summation.

2.3 Two-dimensional toy model and JT gravity

In two dimensions the Einstein-Hilbert action is invariant of topology, due to the Gauss-Bonett theorem, for more details about this see [10, 2]. In two-dimensions every Riemannian metric becomes a solution to the Einstein equations when we set the cosmological constant to zero, this means that the curvature is fixed everywhere and each metric is given the same Boltzmann weight. Finding another solvable, yet interesting action for the Euclidean path integral 4 in two dimensions. A good candidate for this is, according to [10], the Euclidean action. This action has been studied in Jackiw-Teilboim gravity. This model is relevant near extremal black holes, as it captures the dynamics near the horizon of those black holes in higher dimensions.

In Jackiw-Teilboim (JT) gravity the action used in these two dimensions is redefined to the Euclidean action:

$$S = \frac{1}{\kappa} \int d^2x \sqrt{-g} \Phi (R - \Lambda) \tag{6}$$

The Ricci scalar is now directly coupled to a scalar field Φ, which is called the dilation field for historic reasons [10]. The scalar field forces our geometries to have a fixed curvature, which can be hyperbolic, spherical or flat. Most literature (e.g. [**?**, 5, 12]) looks at the case of negative, hyperbolic surfaces, due to its holographic relevance. However we will focus on objects with a flat surface, as this is the simplest case. This allows

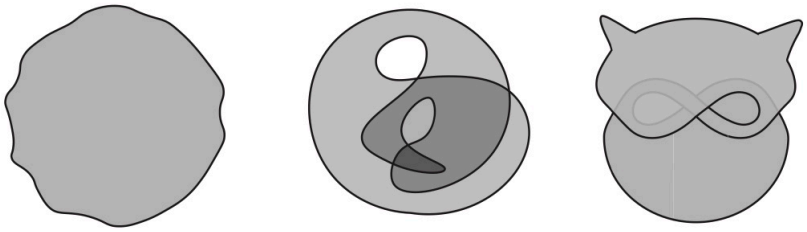

Figure 2: Three intrinsic flat disks. The last two disks have self-overlapping boundaries. The right flat disk is bound by the Milnor curve. *Source [6]*

us to introduce concepts in a simplified context. In JT-gravity the extrinsic curvature of the boundary is allowed to fluctuate as described in [6, 7]. Our interest will lay at the boundaries of the geometries, which are not allowed to diverge immediately. When discussing intrinsic flat surfaces with fluctuating boundaries in two dimensions, flat disks are the most simple objects. As these flat disks are considered random, there is simply not a valid reason to forbid disks from overlapping themselves. Three examples of random flat disks are given in figure 2.

In this thesis we will also look at objects with a higher topology, these are called annuli. Annuli have a second boundary, where certain ideas found for the flat disks do not apply, which we will discuss in chapter 4. In the future, these might be extended to higher boundaries. Here our main goal is to understand $\mathcal{D}g$ in equation 4. We will do this by looking at the basic properties of these surfaces, such as winding number and the length ration between the first and second curve. So it eventually is possible to sum over all surfaces, weight by the correct Boltzman weight.

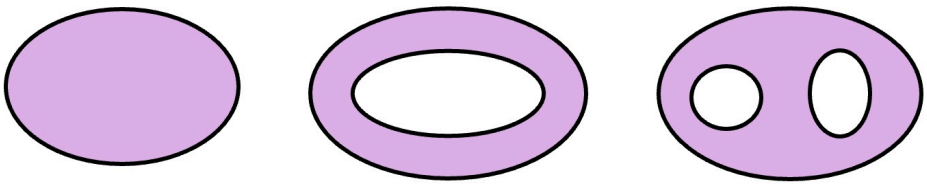

Figure 3: These are different flat surfaces with respectively one, two and three boundaries. In this thesis we will only discuss the objects with either one or two boundaries.

3 Objects with one boundary: flat disks

Before we can look at our objects, annuli, we will first look at the most simple objects in two dimensions: flat disks. A flat disk is an area in $\mathbb{R}^2$ with exactly one boundary. Our goal is still the same, defining the differential of g in the path integral in (4). To reach this goal, we have to describe random disks. Describing random objects is usually done by discretizing the object, which we will do for disks in the next section. This reduces our disks to self-overlapping polygons. We then can fix the sides of the self-overlapping polygons, we call the number of sides n. Then for the good defined[1] subset of these polygons with n fixed sides it is possible to rearrange the order of these sides to create new self-overlapping polygons.

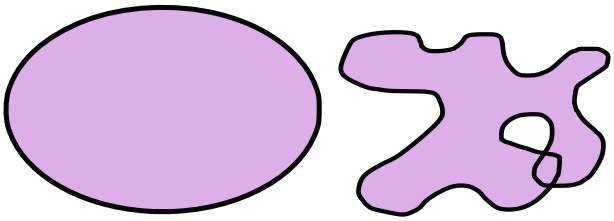

Figure 4: Two random flat disks. The sides of the disks are allowed to overlap.

The main result of this section is that, for any good defined set of n vectors, corresponding to the sides of a self-overlapping polygon, we can find $(n-2)!$ flat disks, which is found by applying an involution, which will be explained in the last part of this section. This section is largely based on the work of Budd in [1].

3.1 Regularization

For a specific combinatorial model of flat disks with a flat Riemannian metric, the properties and statistics have been studied. This model is defined by applying a regularization on flat disks. Regularization is a process that simplifies the solution of a problem that contains a singularity. In the case of flat disks, we regularize the boundary by restricting it to straight sides. This implies that all regularized flat disks are self-overlapping polygons.

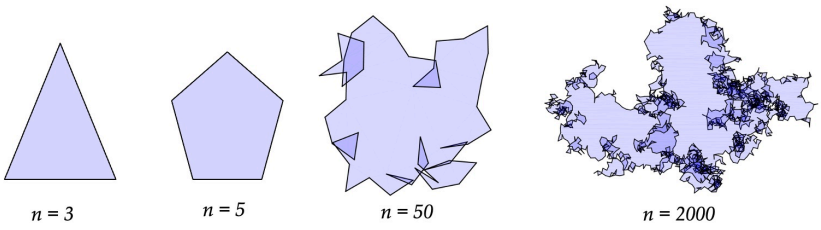

Figure 5: Different discrete flat disks with $3, 5, 50, 2000$ sides. As you can see, disks with more sides definitely have more overlap. *Source: Budd*

[1] Good defined polygons are generic polygons. We will define generic in the next section.

We also assume that the number of sides is finite. We call the number of sides of the flat disk n. This regularization discretizes the flat disks, contrary to the flat disks of figure 4. It is however always possible to take n very large, we expect that the self-overlapping polygons then will go back to complete random flat disks.

We can define the boundary as a closed curve that bends at specific points: $v_1, \ldots, v_n \in \mathbb{R}^2$ where $n \geq 3$. To find truly random points it is possible to sample them from a closed random walk. Using these points, we can form the sides of the flat disk. The side of the disk is the shortest path between v_i and v_{i+1} where $1 \leq i \leq n$. This means that it is possible to write the side of the disk as the difference between two points where the curve bends, $v_{i+1} - v_i$. From this the whole boundary can be constructed as a sequence $Z = \{v_1 - v_n, v_2 - v_1, \ldots, v_n - v_{n-1}\} = \{z_1, \ldots, z_n\}$. This set has cardinality n, which corresponds with the number of sides. When Z is sampled from a closed random walk in $\mathbb{R}^2$ which approaches a Brownian bridge, the cardinality of Z becomes very large, which approaches complete random flat disks again.

Because of the assumption that the inside of every disk is flat, we can define the whole flat disk based on the set Z. Note that the order of the elements in Z is quite important. A small change in the order can construct a different flat disk, or even not a flat disk at all.

3.2 Generic flat disks

Before we go further it is useful to cancel out any particular sets Z which will causes problems later on in this chapter. We do this by requiring Z to be generic. We can call Z generic if Z cannot be partitioned into three subsets which are collinear. In particular, generic Z has no parallel sides. This is better illustrated visually, as seen in figure 6. The sides are shown as vectors. The set Z is generic, because none of the vectors overlap, when all their origins are put at the same point. As we are only ruling out specific cases, we can say that any random set Z is almost surely generic. So all generic sets Z form a subset of full measure of all Z.

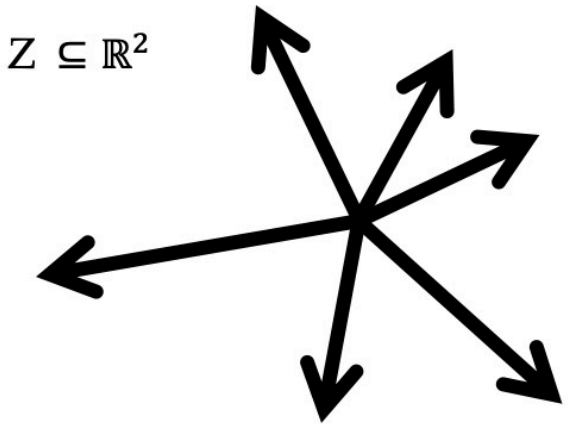

Figure 6: A generic set Z, the set contains 6 elements, these elements can form one convex flat disk and 23 other flat disks

A flat disk is called convex if all angles inside the disk are equal or smaller than π. For any generic set Z we can make exactly one convex flat disk, by putting the elements of the set in a specific order, to be precise, counter clockwise. This is true for any generic set Z. This is not the only flat disk we can form from this set. It is possible to switch the order of the elements in Z to find other flat disks. The paper mentioned earlier has proved the following theorem:

Theorem 3.1. *(Budd, 2024) If Z is generic, then the number of n-sided flat disks with side set Z is $(n-2)!$.*

This states that the number of unique flat disks made from Z is only dependent on the cardinality of Z, which is the number of sides. In the next sections, we will look at a few key elements used in this proof. These elements will be useful for the next chapter, where we will be looking at different ways of counting flat discrete annuli.

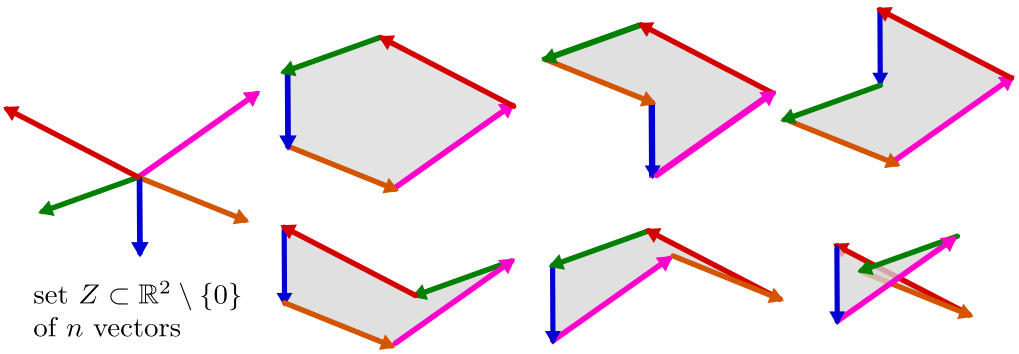

Figure 7: For $n = 5$, we can exactly create $(5-2)! = 6$ different flat disks, according to theorem 3.1. The upper left disk is the only convex flat disk, the other flat disks have at least one angle larger then π. The disk on the lower left is the one with self-overlap. *Source: Budd*

3.3 Diagonalizing flat disks

As mentioned above, for any generic set Z, there is a unique convex flat disk. Every other flat disk must have at least one interior angle larger than π. To understand why only the cardinality of Z is sufficient to find the number of allowed flat disks, we would like to get rid of the interior angles that are larger than π. If this condition is satisfied, the disk is called a convex diagonalized flat disk.

For any flat disk D we can define a convex diagonalization Δ. This diagonalization is a collection of pairwise non-intersecting diagonals, whose cardinality we denote by $|\Delta|$. The cardinality is the number of diagonals used in the disk, for the disk to be convex diagonalized[2]. The diagonals create *subpolygons* inside the flat disk. Each flat disk D has a collection of convex diagonalizations, which is illustrated in figure 8. Each of these diagonalizations can be labelled based on the number of diagonals, $|\Delta|$. We call this label Λ.

$$\Lambda_\Delta = (-1)^{|\Delta|-(n-3)} \tag{7}$$

[2]These convex diagonalizations are useful to distinguish different flat disks. As distinct flat disks can have the same order of elements $z_1, \ldots, z_n$, but cannot share the same convex diagonalizations. A nice example is the Milnor Curve, which is discussed in [7, section 3.4].

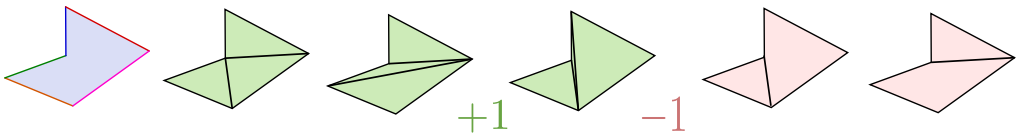

Figure 8: All possible diagonalizations of a flat disk from the $n = 5$ example. The allowed diagonalizations are labelled by equation (7). When we sum over all Λ corresponding to this disk the outcome is exactly 1. *Source: Budd*

Λ has only values of plus or minus one. This means that the exponent of equation (7) must be even for all diagonalizations where the maximum number of diagonals is used. A flat disk with n sides has a maximum of $n-3$ diagonals. Therefore, the sum over all Λ of one flat disk is always $+1$, as we required that for each flat disk there is always one diagonalization more possible with a positive sign than a negative sign. This statement is proven in [1] using algebraic topology arguments.

From this we can conclude that the number of flat disks that can be created from a generic set Z is equal to the sum of the labels of all convex diagonalizations made in the disks formed by Z. This also holds for any individual flat disk. This implies that we still can go back to the continuous disk and the number of disks we count remains equal.

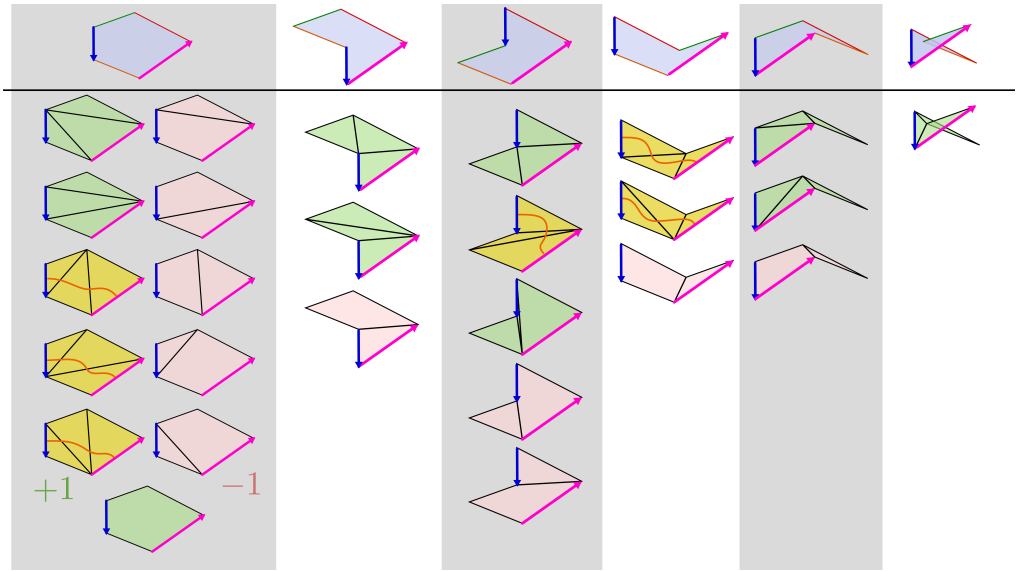

Figure 9: These are all possible diagonalizations of the $n = 5$ example, all diagonalizations are labelled and two favourite vectors are marked. All yellow disks cannot be crossed out against another disk, as their subpolygons are all triangles and a path between the two favourite vectors can be drawn. *Source: Budd*

3.4 Involution

The next step in counting flat disks is by the use of an involution. In general, an involution is a mapping which is the identity when applied twice. We can create an involution that maps diagonalizations marked with a $+1$-label to diagonalizations with a -1-label.

This involution leaves certain +1-labelled diagonalizations invariant. The number of invariant diagonalizations equals the number of unique flat disks. This makes the involution a very useful tool for counting flat disks.

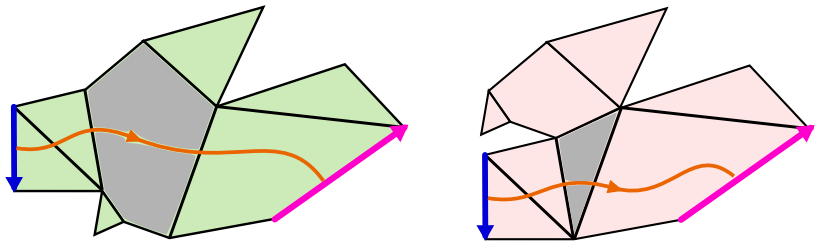

Figure 10: Two random flat disks that are crossed out by the involution. The left flat disk is crossed out because one of the subpolygons, marked grey, is not a triangle. In the left flat disk the grey subpolygon has no side adjacent to the boundary, so no side is an element of Z. *Source: Budd*

When we have found all possible convex diagonalizations for a given set Z and want to define the involution, we have to choose two favourite sides from Z. These can be picked at arbitrarily, but cannot be the same side, let them be z_1 and z_2. Between those sides we can draw a path through the polygon. A diagonalization can be crossed out against another diagonalization if it either has subpolygons that are not a triangle or if one of the subpolygons has no sides that are an element of Z. We only look at the problem we encounter first when following the path between our two favourite sides. An example of both cases can be found in figure 10.

The involution itself switches the order of two subsequences of Z. When we switch these two subsets again we get the original figure back. This aligns with the definition of an involution. These subsequences consist of one or multiple vectors. Notice that certain subsequence create a diagonal inside the polygon. For example, the large green vector in figure 11. This vector is the sum of two vectors on the outside that belong to Z. In this figure two subsequence are switched. One subsequence is the yellow and mint coloured vector, where the yellow vector is a sum of two vectors in Z. The other subsequence is the blue vector. When we switch those sequences we also have to add another diagonal to for our polygon to remain convex. Therefore the second diagonalization has an opposite label.

We can now apply this to every convex diagonalizations found in our $n = 5$ example, which causes most diagonalizations to cancel out each other. Only *neat triangulated convex diagonalizations of polygons with generic sides* remain. They only consist of triangle subpolygons with exactly one side of the subpolygon corresponding to one vector in Z, which are all marked yellow in figure 9. Notice that they do not necessarily represent all possible flat disks formed by the set Z. The number of diagonalizations that remain invariant, is however the same.

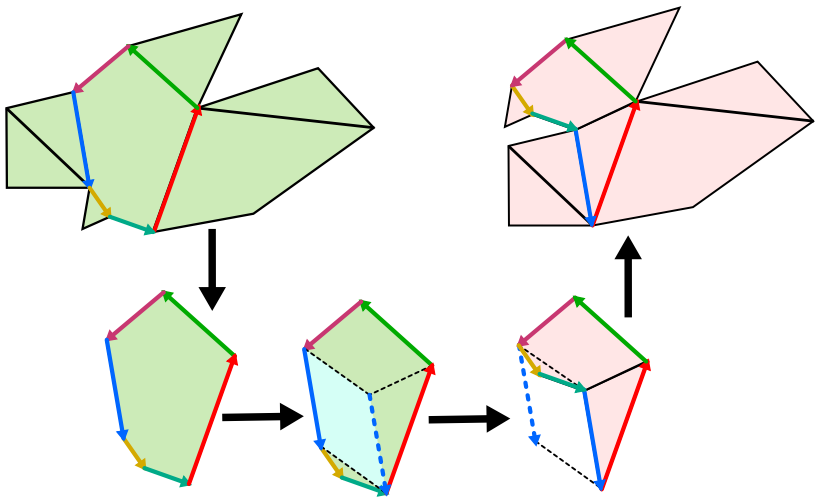

Figure 11: Two diagonalizations that map to each other when applying the involution. Notice that switch of the two subsequences gives the polygon an interior angle larger than π. Therefore an extra diagonal is necessary, causing the polygon to change from a $+1$ to a -1 label. *Source: Budd*

3.5 Counting flat disks

We now can conclude that the number of *neat triangulated convex diagonalizations of polygons* created of generic Z corresponds exactly to the number of flat disks created from Z. This was our goal, as we can represent each *neat triangulated convex diagonalization* as a unique closed walk with n steps – the corresponding algorithm is the same as for annuli, we will discuss this algorithm in chapter 4. So we can now count the possible walks of n steps instead of the flat disks. Recall from the previous section that we had chosen two favourite sides to apply the involution. These two sides are the only sides which cannot change location in the closed walk. Which means that for n steps and two favourite sides that cannot change location we have $(n-2)!$ ways of constructing the random walk. Therefore, we can conclude that theorem 3.1 is true.[3]

[3] A more abstract proof using generating functions can be found in [1].

4 Including an extra boundary: annuli

4.1 Regularization of an annulus

Now, we can analyse two dimensional flat objects with an extra boundary: annuli. The most trivial annuli are ring-shaped, however in section 4.3 we will see that certain other well-known figures are topological equivalent to an annulus. Similarly as for the disks, we will only look at the boundary and assume the inside is flat, or in other words, has a flat Riemannian metric. However, we first have to regularize the annuli. This works the same as for the flat disks.

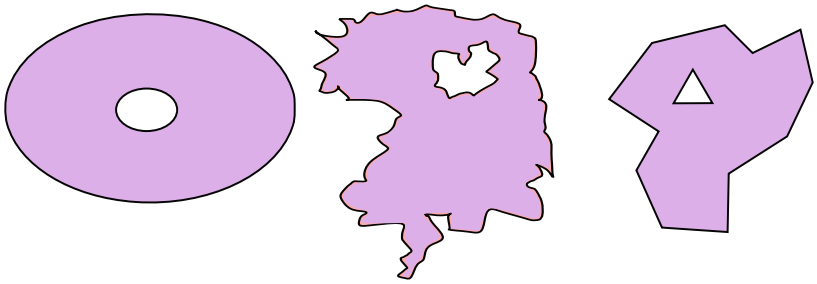

Figure 12: Three different annuli. Only the one on the right is regularized, as this is the only one with a finite number of straight lines as a boundary.

The boundaries of an annulus can also be defined by a set of points $v_1, \ldots, v_n \in \mathbb{R}^2$. We can form the first curve with the points $v_1, \ldots, v_{i-1}$. Then the second curve is defined by the points $v_i, \ldots, v_n$, see figure 13.

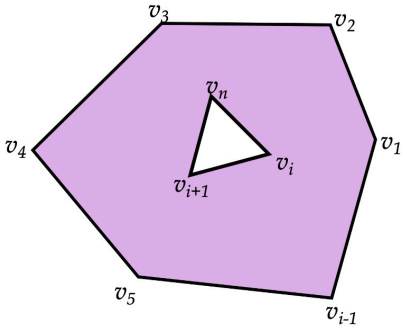

Figure 13: The bending points of an annulus with $n = 9$ and $i = 7$.

We can define all the sides by taking the shortest path between two points, which we denote as $v_1 - v_{i-1} = z_1$. This works the same as the method we have described for flat disks, until the i^{th}-element. The points $v_i, \ldots, v_n$ belong to the second curve, the last side of the first curve is then described by $v_{i-1} - v_{i-2} = z_{i-1}$ and the first element of the second curve by $v_i - v_n = z_i$. Now we can construct the whole annulus by the set Z':

$$Z' = \{v_1 - v_{i-1}, v_2 - v_1, \ldots, v_{i-1} - v_{i-2}, v_i - v_n, \ldots, v_n - v_{n-1}\} = \{z_1, \ldots, z_i \ldots, z_n\} \quad (8)$$

Notice that this set still has cardinality n. We can always let this cardinality diverge again, just as with disks, to get truly random annuli back. It is also still possible to create different annuli by changing the order of elements in Z'. As we are following the same steps as the previous chapter, it would logical to now define a similar theorem for generic on annuli. We will do this in section 4.3, but first we have to adjust our view of counting. The addition of the second boundary adds another parameter to our problem, as we have to keep in mind that the location of the second curve can change, creating a new annulus.

We can now discuss the main goal of this thesis. Which is finding, for a given generic set Z', the possible n-sided flat annuli. The best would be if this would be a number which only depends on the cardinality of Z'. However, the extra parameter might cause certain difficulties. To reach this goal, we have to look at the properties of the just defined annuli, and try to find a similar bijection to a closed walk with n steps.

4.2 Moduli space of an annulus

As briefly mentioned before, for a given set Z' we can still make an uncountable number of annuli, since it is not fully defined where the second curve is located. So even if we move the second curve an infinitesimal amount, we get another annulus. This makes the number of annuli that can be formed by a generic[4] set Z' uncountable. Therefore, we should not look for a number of annuli, but the volume of a moduli space.

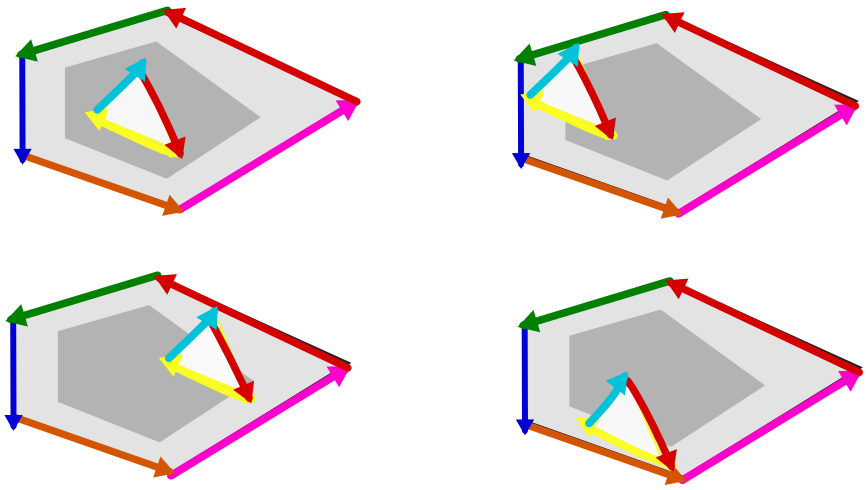

Figure 14: These are four different annuli, made from the same sequence of elements in Z'. We can make infinitely more of them, as long as the centre point of the second curve is inside the grey area. This makes the grey area a component of the moduli space for the given sequence of Z'.

In mathematics, a moduli space is a geometric space of solutions [8]. There are several related concepts which can be called moduli spaces; here we use the term moduli spaces which in literature is also named *fine moduli spaces*. We have a space where each point

[4]We will define generic on annuli in section 4.3

in this space corresponds to a solution. We can represent this moduli space visually, as done in figure 14. The darker grey area represents the component of the moduli space of this annulus, as each point in this area is a point where the middle of the second curve can be located. This makes the grey area equivalent to the moduli space corresponding to a certain sequence of Z'. As this is a volume instead of a number we have to change our view on counting annuli. Meaning, we stop looking for a number but start looking for an area of the two-dimensional moduli space. This moduli area will weigh each possible sequence of Z'. Summing over all orderings of Z', this gives the volume of the moduli space of Z'. In the next sections we will try to find a similar bijection to a closed walk as for disks, keeping in mind that we are looking for a volume of the moduli space.

4.3 Generic annuli

As mentioned before, we can call a set Z' generic, if Z' cannot be partitioned in three non-zero subsets: $I_1 = I_2 = I_3$, as defined before for disks. Intuitively, you might think that every annulus can be partitioned into three non-zero subsets. This is the case for all the annuli we have seen in figures until now. The subsets would be, for example, I_1 the second curve, I_2 the first half of the first curve, and I_3 the second half of the first curve. However, for a real generic annulus this is not the case. We have to remove all non-generic annuli, this does not cause any problems, as generic annuli form a full measure subset.

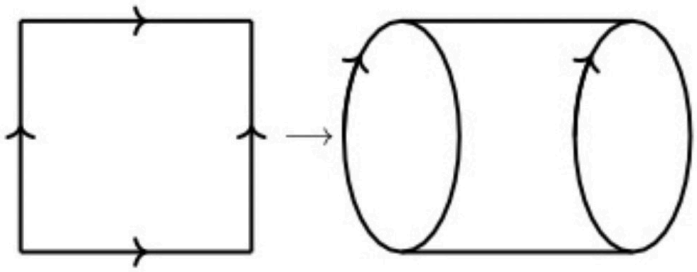

Figure 15: By identifying sides we can also create new figures with higher boundaries. Two sides are glued together, or become identified, creating the cylinder in the figure. A cylinder is an annulus. *Source: [13]*

Previously, we only constructed annuli by cutting a hole into a flat disk. We can, however, also construct generic annuli by glueing certain edges of a surface together. An example of this can be found in figure 15. These surfaces are, when glued together, from a topological perspective also annuli [11]. Those sides that are glued together are now the same diagonal. We will call this diagonal an identified diagonal δ_i. In figure 16, we can see various other *generic* annuli.

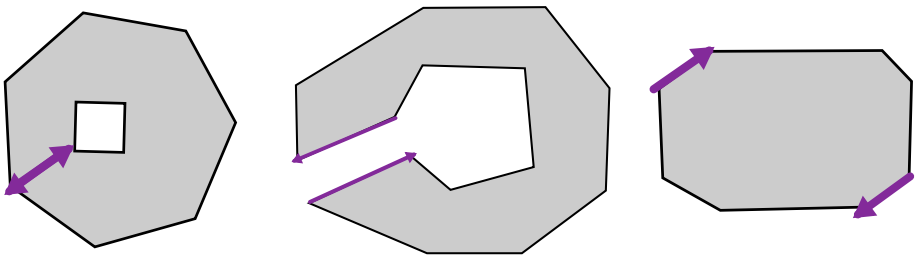

Figure 16: These are three different annuli with an identified diagonal δ_i. The annulus on the left can be divided into three equal subsets, and is therefore non-generic.

From a mathematical perspective, we can say these annuli have a non-zero holonomy. When we start from the identified diagonal and walk along the annulus till we get to the other vector of δ_i. We will arrive at the same point in the annulus, but this is not the same point in space. Which means this annulus has a non-zero holonomy. This differs from the annuli we saw previously, they all had a zero holonomy. In these zero holonomy annuli we could easily create three equivalent subsets, making them non-generic. Often the next steps can just as well be applied to non-generic annuli, only in some cases this can lead to degenerate situations. Therefore, we keep using zero holonomy annuli as our examples, even though they are not generic, since they are easier to visualize.

Another property of annuli which is useful to mention briefly is the turning number of an annulus. The turning number is defined as the total curvature of the first curve divided by 2π [3]. Because random annuli are allowed to self-overlap or due to non-zero holonomy their turning number can increase. In this thesis we will restrict the turning number to an integer.

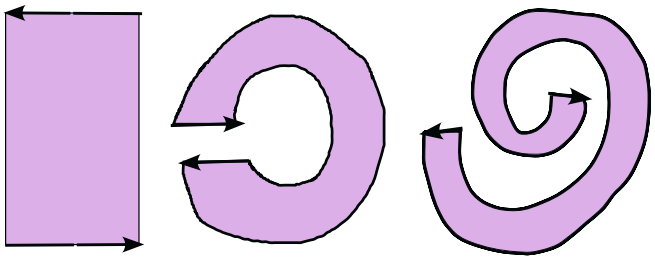

Figure 17: Three annuli with different turning numbers. The annulus on the left has turning number 0, the middle one has turning number 1, and the last annulus has turning number 2.

4.4 Diagonalizing annuli and the Involution

Now we have defined the moduli space of an annulus, we can start counting the number of possible sequences. We would like to apply the involution from disks again, to find a similar bijection to a closed walk. Therefore the annuli need to consists of only convex subpolygons. Every non-trivial annulus has at least one internal angle larger than π. So we have to diagonalize them all, creating convex subpolygons. This can be done in various ways, see figure 18. If the annulus has an identified side δ_i, this side counts as just one diagonal.

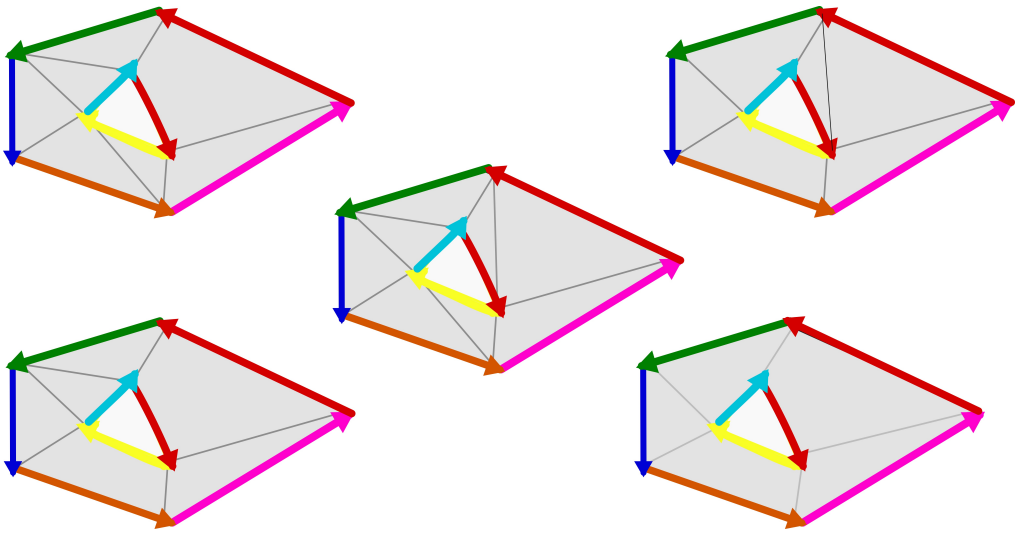

Figure 18: These are five of the possible ways of convex diagonalizing the same annulus. When applying equation (9), the upper left and down right annulus get the label -1, because they have an odd number of diagonals. The others get the $+1$-label.

Just as we did in the previous chapter, we can use the cardinality of each diagonalization $|\Delta|$, which stands for the number of diagonals used, to label each diagonalization Δ. We have to redefine the formula (7) from chapter 3.3. As this formula depends on the maximum number of non-intersecting diagonals possible. For disks this maximum is $n-3$, however for annuli the maximum number equals the number of sides n. This gives us the formula:

$$\Lambda_\Delta = (-1)^{|\Delta|-n}. \tag{9}$$

We then sum again over all Λ_Δ corresponding to a specific annulus, which always sums to exactly one. This based on the same proof using algebraic topology arguments as mentioned in section 3.3. Now we have labelled each convex diagonalized annulus, and apply the involution on annuli in the next section, so that we eventually can find a bijection to a closed walk.

We then apply the involution on annuli. There is only one main difference: instead of choosing two favourite sides as we did with flat disks, we now choose one of the diagonals arbitrarily. We can then draw a path through the annulus which ends at our favourite diagonal. The first non-triangle shaped subpolygon we will encounter will again be turned into an triangle without a side adjacent to the boundary, by adding a vector. If we first encounter a triangle with no side adjacent to the boundary, one of its sides will be removed, creating a non-triangle subpolygon. This is the same method as for disks, discussed in section 3.4. All annuli with the -1-label are converted to an annulus with a $+1$ label with this method. If this path only crosses triangle shaped subpolygons and there are no subpolygons left, this diagonalization is invariant under the involution. We call these annuli *neat triangulated*. So instead of counting all diagonalizations it is sufficient to only count the neat triangulated annuli. In figure 18 the annulus in the middle is *neat triangulated*. We are now left with the annuli that are invariant under the involution, which exactly corresponds to the amount of annuli that can be created from Z'.

4.5 Annulus to a closed walk

The great benefit of neat triangulated annuli is that we can represent them all as a closed walk with $(n+1)$-steps. The extra step will be the identified diagonal δ_i, if there are no identified sides it can be an arbitrary diagonal. If we choose another diagonal from the annulus we get the almost the same walk, only the starting line will differ. The starting line originates at the point of origin p_o, even though the starting line can change, the point of origin can not. From this first line we will move counter-clockwise along the annulus, as seen in figure 19, encountering each subpolygon in the annulus. Because the annuli are neat triangulated, we will find exactly one vector belonging to Z' in every subpolygon. Then we put all vectors we encountered back to back. If we have done this right we will end up back at the end of the first line, the identified diagonal.

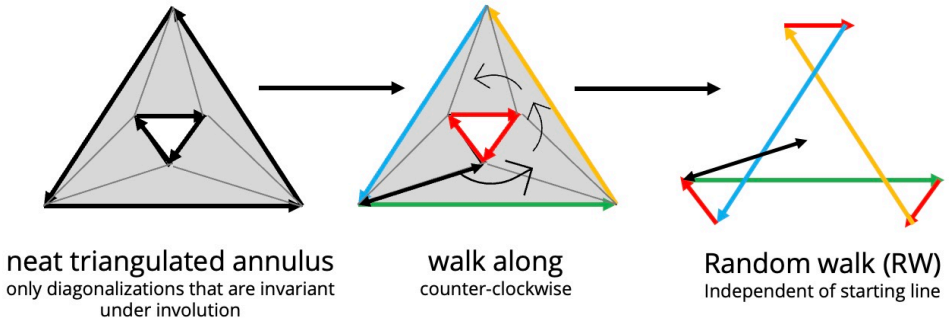

Figure 19: This is the method converting an annulus to a random walk. This only works for *neat triangulated* annuli, otherwise there is no clear order of placing the vectors. We choose to walk counter clockwise as the vectors are also oriented this way. The point of origin p_o is located in the middle of the closed walk. Notice that this annulus is not generic, however this does not create any issues.

For each closed walk we can define different winding sectors. According to [4], each point in the sector is being labelled by the winding number w, which represents the number of times the curve bends counter-clockwise around the specific point. In figure 20 we find an example of the different winding sectors of a general curve. The area outside the curve has winding number zero. This zero-sector differs as it mostly consists of an infinite part. Notice in the figure that there is also a zero sector embedded in the curve.

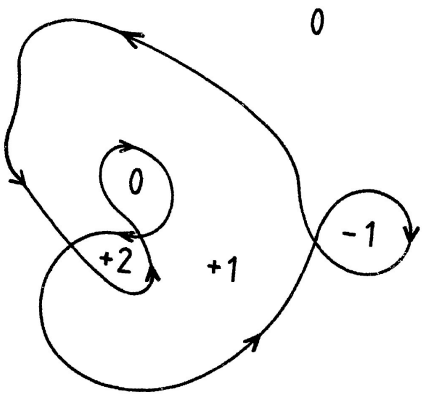

Figure 20: A closed curve with different winding sectors. Each sector is labelled by its winding number w. Notice that area of the zero sector is infinite. *Source: [4]*

Something that catches our eye, when applying this method to various generic annuli, is the fact that the moduli space is already visible in an annulus, see figure 21. More precisely, the area in the random walk with winding number $+1$, corresponds exactly to the moduli space of an annulus with turning number 1. This statement can even be generalised. When an annulus with a turning number is converted to a closed walk, the area of the walk with the corresponding winding number w corresponds to the moduli space of the annulus. Therefore, if we want to sample a random flat annulus with n, it is sufficient to create a random closed walk with n-steps and a point of origin p_o. This point lies in a sector winding number w, which determines the turning number and moduli space of the corresponding flat annulus.

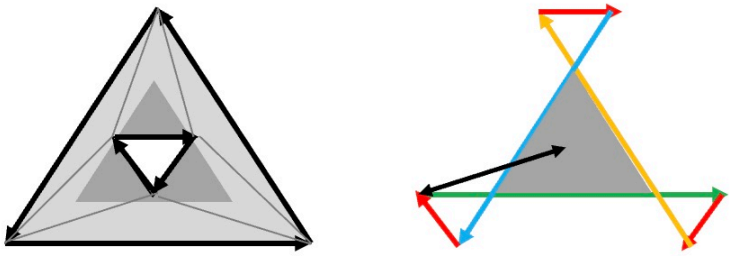

Figure 21: As clearly visible, the moduli space of the neat triangulated annulus matches the middle surface in the closed random walk. This is the surface with a positive winding number, which is very convenient, as these surfaces have already been studied in [4].

These areas strongly depend on Z', and unfortunately there does not yet exist a formula to calculate the area of the moduli space. However, if we take Z' random and the number of sides very large, the corresponding close walk will approach a Brownian bridge. This is quite interesting, as the areas of a Brownian excursion already have been studied in [4]. This paper concludes that the area with winding number w inside the random walk has the average size of $\frac{\tau}{(2\pi w)^2}$. Where τ is a scaling of the closed walk which we can choose to set to one.

If we look with a bit more detail to the closed walk we can also see which vectors belong to the first and second curve of the annulus. We do this by using the point of origin p_o. From this point we draw a line to the start of a specific vector, see figure 22. Now, based on this line and the vector we can determine if the vector belongs to the first or second curve. If the vector points left, viewed from the line, it belongs to the first curve. This is the case in the figure. If it points right, the vector is part of the second curve. It is possible to use this method for any closed walk with $(n+1)$-steps.

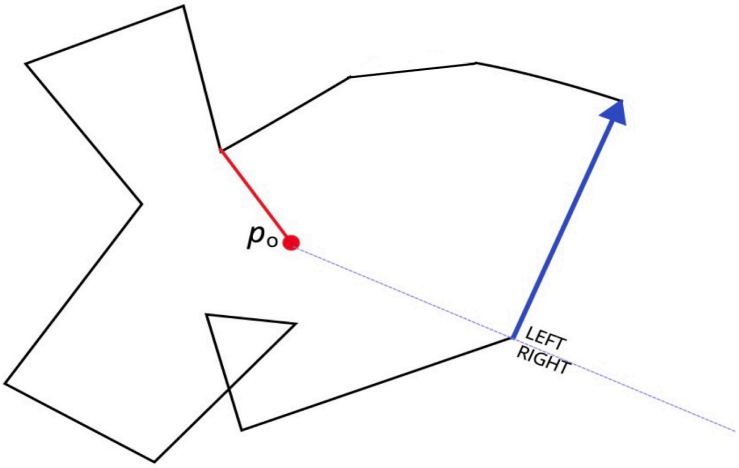

Figure 22: A closed walk that represents an annulus. The red dot is the point of origin p_o and the red line the starting line of the closed walk. In this walk we can determine if each vector belongs to the first of second curve. For example, the blue vector belongs to the first curve, as the angle between the vector and drawn line is larger than π.

Hence, we can already determine which vectors belong to the first curve and which vectors belong to the second curve in the closed walk. This makes it possible to start finding statistics on length of both curves and their ratio, without converting each closed walk to an annulus. However, as we are working with the *neat triangulated annuli*, these statistics are not valid. Certain unique annuli are cancelled by the involution, see figure 9 in chapter 3. Therefore an problem that remains open is the possibility of following a single vector through the involution. This is necessary as it allows us to perform statistics on the curves of an annulus. This ratio would give us insight in the shapes of truly random annuli. These are annuli sampled from completely random walk. It is however already possible to do this when we weigh each annulus with the number of neat triangulations it admits.

5 Conclusion and outlook

We now can conclude that for a given generic set Z', the number of annuli we can make scales with the area of the moduli space of each neat triangulated annulus and the number of neat triangulated annuli. The number of neat triangulated annuli is equal to the number of annuli that each have a different moduli space. Therefore, we can conclude that for a given generic set Z' we can find a set of n-sided flat annuli, however this set does not only depend on the cardinality of n. For flat disks the solution was an exact number, $(n-2)!$, this is not the case for annuli. For annuli, we have to look at the moduli area of each allowed sequence of Z'. These areas weigh every sequence of Z', therefore the solution must be a moduli space in three dimensions.

When we represent each annulus as a closed walk with $(n+1)$-steps, we have found that the moduli area of the annulus corresponds to the area in this walk with the same winding number, w, as the turning number of the annulus. These winding areas have been studied previously and are proportional to $\frac{\tau}{(2\pi\, w)^2}$, which is dependent on the distances inside the random walk and therefore, dependent on the specific elements in Z'.

However, many research questions remain open. An example is the ratio between the both curves in the annulus, especially for larger side sets. We have found an algorithm to determine if a vector belongs to the first or second curve, however this only works for *neat triangulated annuli*. This raises the question if it is possible to follow a single vector through the involution, which would make it possible to study this ratio without weighing it to the number of neat triangulation an annulus admits.
In this thesis we already have applied some generalizations to the methods used for counting flat disks. For example, the labelling and involution. It might be useful to look if these generalizations still be useful for objects with higher topologies. We expect that for objects with three boundaries the idea of diagonalizations and involution still would work, however, there might be difficulties by representing these objects as closed walks. The solution would still be a moduli space in three or four dimensions. Even though we cannot yet completely define $\mathcal{D}g$ from the Euclidean quantum gravity integral in equation (4), the next step could be starting various simulations of annuli with large side set. Perhaps, this could give us more insight on the ratio between the curves.

Acknowledgements

I would like to thank my supervisors, Bart Zonneveld and Timothy Budd, for their guidance and support throughout my internship. I really enjoyed learning about two-dimensional quantum gravity and looked forward to our weekly meetings. I'm grateful for the opportunity to do a theoretical internship.
I would also like to thank my friends for their support during my internship, especially at the Winter Symposium and for proofreading my thesis. Finally, I'd like to thank Wim Beenakker for being the second reader of this thesis.

References

[1] Timothy Budd. Enumeration and statistics of flat disks. Private document, version March 2024.

[2] Timothy Budd. Lessons from the mathematics of two-dimensional euclidean quantum gravity, 2022. arXiv:2212.03031.

[3] Manfredo P. Do Carmo. *Differential Geometry of Curves and Surfaces*. Pearson, February 1976.

[4] A. Comtet, J. Desbois, and S. Ouvry. Winding of planar brownian curves. *IPN Orsay Preprint*, (IPNO/TH 90-02), January 1990.

[5] A. Comtet and P. J. Houston. Effective action on the hyperbolic plane in a constant external field. *Journal of Mathematical Physics*, 1985.

[6] Frank Ferrari. Jackiw-teitelboim gravity, random disks of constant curvature, self-overlapping curves and liouville CFT_1, 2024. arXiv:2402.08052.

[7] Frank Ferrari. Random disks of constant curvature: The lattice story, 2024. arXiv:2406.06875.

[8] Joe Harris and Ian Morrison. *Moduli of Curves*. Graduate Texts in Mathematics. Springer, New York, NY, July 1998.

[9] Thomas Hartman. *Lectures on Quantum Gravity and Black Holes*. Cornell University, 2015.

[10] Thomas G. Mertens and Gustavo J. Turiaci. Solvable models of quantum black holes: A review on jackiw-teitelboim gravity, 2022. arXiv:2210.10846.

[11] James R. Munkres. *Topology*. Pearson Education Limited, 2nd edition, 2013.

[12] Phil Saad, Stephen H. Shenker, and Douglas Stanford. Jt gravity as a matrix integral, 2019. arXiv:1903.11115.

[13] Steffen Sagave. *Lecture Notes on Topology*. Radboud University Nijmegen, April 2024.